Environment, Development and Sustainability
https://doi.org/10.1007/s10668-020-00986-6

Integrated assessment of extreme events and hydrological responses of Indo-Nepal Gandak River Basin

Pawan K. Chaubey[1] · Prashant K. Srivastava[1] · Akhilesh Gupta[2] · R. K. Mall[1]

Received: 15 November 2019 / Accepted: 15 September 2020

Abstract
Changes in climate cause significant alterations in morphometric parameters and may lead to hydro-meteorological hazards. In this study, an attempt has been made to identify drainage morphometric characteristics through topographic, geologic and hydrological information to assess the extreme weather events (flood) over the Gandak River Basin (GRB). The standardized precipitation index (SPI) and rainfall anomaly index (RAI) were used for deducing extreme rainfall incidences derived from the Tropical Rainfall Measuring Mission precipitation datasets. An assembled frequency distribution as well as trends in RAI and SPI was calculated to understand the hydro-climatological behaviour of the basin. During the monsoon season, the years 1998, 2007, 2011, 2013 and 2017 witnessed the extreme flood events. The variations in heavy and intense rainfall in short time can be linked to extreme flood events, which leads to channel shifting and modifications, can be deduced from provided asymmetric factors and sinuosity index. The results illustrated that both the monsoonal rainfall and the frequency of extreme rainfall over the basin are increasing, which could be a reason for a high severity and frequency of flood events in the GRB.

Keywords Flood · Standardized precipitation index (SPI) · Rainfall anomaly index (RAI) · Morphometric · Gandak basin (Indo-Nepal region)

1 Introduction

The Indo-Gangetic Basin (IGB) comprises several river streams and act as an important source for freshwater resources in the Indian region. The extreme rainfall events during South-west monsoon are mainly driven by Himalayan mountain ranges over Indo-Nepal regions in south-central Asia (Singh and Mal 2014; Mall and Srivastava 2012). Gandak River Basin (or GRB) holds a unique topography covered by glaciers snowfields and the mountainous terrain over the Nepal, while the downstream area forms an alluvial plain in India. Because of the complex nature of the mountainous ecosystem, it is often

✉ R. K. Mall
rkmall@bhu.ac.in

[1] DST-Mahamana Centre of Excellence in Climate Change Research, Institute of Environment and Sustainable Development, Banaras Hindu University, Varanasi 221005, India

[2] Department of Science and Technology, New Delhi, India

Published online: 24 September 2020

problematic to understand the hydrological responses and extreme precipitation events of GRB.

In the past, many researchers documented the use of morphometric analysis for extreme event management as well as designing control measurements for flood and drought, etc. (Pophare and Balpande 2014; Choudhari et al. 2018; Nagalapalli et al. 2019; Mall et al. 2019). Morphometric is the analysis of the mathematical measurement of the earth's surface, shape and dimension (Clarke 1966). Analysis of quantitative morphometric parameters provides the information about the hydrological process and nature of topography in the basin (Mall 2013; Kumar et al. 2018; Pradhan et al. 2018). Evidence of topographical and hydro-geological characteristic can be described by the drainage morphometric parameters, which is valuable for water resources potential assessment and management (Pophare and Balpande 2014; Shukla et al. 2014; Yadav et al. 2014; Chaubey et al. 2019). Chaubey et al. 2019 examined meteorological extreme by applying statistical multi-scalar indices and moreover established a relation between quantitative drainage characteristics with LULC changes in the river basin. Generally, the drainage system represents the subsurface lithology as well as predominated topographic features, whereas river morphology comes under the modification of river streams along its cross section owing to its erosion and sedimentation over the channel network (Pophare and Balpande 2014). Transverse topography asymmetry (T) and asymmetry factor (AF) can be used to examine the shifting of river channel (Stankevich et al. 2020).

Precipitation and soil moisture are the essential parameters for characterizing the basin in terms of their hydrological responses for water resources management (Mall et al. 2006; Gupta et al. 2013; Bhatt and Mall 2015; Edon and Singh 2019; Dey et al. 2020; Singh et al. 2020). The study may assist for water resources management with suitable planning and design for a kind of pre-requisite river morphology (Horton 1945; Miller 1953; Chaubey et al. 2019). The past studies have used different climate indices for spatio-temporal variation for establishing annual and seasonal period of drought over the central part of Nepal region (Sigdel and Ikeda 2010; Dahal et al. 2016). Several challenges were taken as per their study for the society, viz. health hazard, crop damages, flood, water contamination, soil erosion that were caused by extreme rainfall events (Rajeevan et al. 2008; Mall et al. 2011, b). Thus, the Gandak catchment has faced severe extreme precipitation (flood) events in last two decades in various districts covering both India and Nepal, which has caused loss to the properties and cost millions of lives.

There was an increasing awareness about the flood conditions and its control through approaches based on morphological studies and precipitation (Stankevich et al. 2020). As per Malik et al. (2020), trend of extreme precipitation events can also be evaluated by using appropriate global circulation model (GCM). According to McKee et al. (1993), SPI is an important tool for monitoring the rainfall variation in the aspect of flood situation over a region. Many researchers adopted the SPI for flood monitoring with monthly precipitation as an input on the shorter timescales as 1, 3 and 6 months and also used for development of soil saturation and water resources management (Seiler et al. 2002; Deo et al. 2015). Researchers also used the long-term rainfall data for the river basin to study the probabilistic interpretation, in decision making and risk assessment for flood-drought (Dahal et al. 2016; Meshram et al. 2018).Therefore, an integrated approach is needed by evaluating extreme weather events and geomorphology to reveal flooding in

the study area. This study is an attempt to evaluate the usefulness of SPI (McKee et al. 1993) and RAI (Rooy 1965) for analysis of extreme precipitation events in the GRB. Furthermore, the morphometric parameters that could be responsible for extreme events in the basin were also provided along with the nonparametric Mann–Kendall's test for understanding the trend and pattern in the data.

2 Study area

The GRB comprises Gandak and its six sub-watersheds, flowing north to south-east above the northern Gangetic plain. GRB originates at the Tibetan Plateau from Nhubine Himal Glacier from Nepal and confluences in India (Fig. 1). The total length up to its confluence after flows south-east, and then it connects with the Ganges near Patna district with downstream of Hajipur at Sonepur (Bihar, India) after travelling 15,846.08 km. in length (Fig. 1). GRB is controlled by the High Mountainous or Himalaya ranges and South Asian Monsoons. The basin shows a steep variation of weather due to the presence of mountainous peaks of Langtang, Machhapuchhre, Dhawalagiri and Annapurna. GRB has diverse geological record ranging from Cretaceous-Tertiary igneous and metamorphic rock followed by Precambrian rocks to Quaternary sediments in the lower south-east (SE) part of basin.

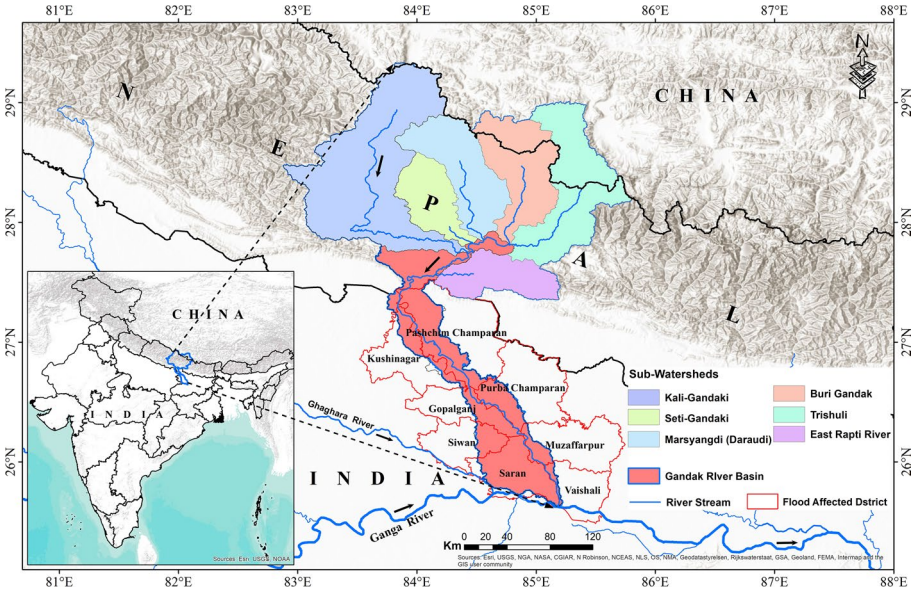

Fig. 1 Geographical location of the study area

3 Material and methods

3.1 Datasets

3.1.1 Precipitation and DEM

The morphometric analysis and delineation of drainage network were carried out by the Shuttle Radar Topography Mission (SRTM) with 90 m spatial resolution in GIS environment (https://srtm.csi.cgiar.org). The SRTM uses interferometric synthetic aperture radar (InSAR), which measures earth's elevation using two radar antennas and a single pass (Szabó et al. 2015; Rawat et al. 2018). The volumetric rainfall has been extracted for GRB and its six sub-watersheds over the Indo-Nepal region using 21 years of precipitation dataset taken from NASA Earth Observation (https://pmm.nasa.gov/data-access/downloads/trmm or https://disc.gsfc.nasa.gov). This dataset is a combined Multi-satellite Precipitation Analysis (TMPA) mission of Japan (JAXA) and USA (NASA) that provides global tropical rainfall data at 0.25° X 0.25° spatial resolution (Malik et al. 2020).

3.1.2 Land use/land cover, soil and geology

Human activities (deforestation) cause transformation of LULC and are responsible for landscapes alteration and geographical occurrence of flood (Abdulkareem et al. 2018). Satellite remote sensing has been used to examine the classification of LULC changes as all spatial and temporal scales over the study area (Singh et al. 2018; Chaubey et al. 2019). The satellite-derived LULC derived from LANDSAT-7 (https://earthexplorer.usgs.gov/) is showing snow and forest cover in the Nepal region while agricultural land can be observed in the Indian side (Fig. 2).

Figure 3 shows the soil and geological feature of GRB has been extracted from Harmonized World Soil Database v 1.2 (https://www.fao.org/soils-portal/soil-survey/soil-maps-and-databases) and Global Geology dataset from ESRI-USGS, respectively. Most of the area of GRB is found covered by undivided Precambrian (37%) rock, quaternary sediments (22.18%) of the mountain sedimentary mud and gravel in the north-eastern (NE) part of upper Gangetic plain (India). A very less area was covered by typical Paleozoic rocks (1.91%) and Mesozoic igneous rocks (1.01%) over mountain ridges. Geology of Gandak River is unique, and it was formed due to the collision of Southern Gondwana land and Northern Eurasian land with the sediments of Tethys Sea. The study area is showing widely different formations in southern and northern parts of Nepal region. In addition, the crystalline formations of the Archean iscovered by the alluvium of Terai. The sedimentary deposits are due to the formation of a giant mountain as well as Siwalik through the east–west river gradient (NIH-Roorkee 2017). The Gandak catchment area was geologically dominated by the alluvium followed through Jurassic with Triassic formations (Dwivedi et al. 1997). Moreover, the river basin was considered as a flood basin in between the Burhi Gandak River and Kosi River, which were tectonically active with predominant regional structure (Mohindra et al. 1992). Figure 3 shows the main frontal thrust (MFT) and main central thrust (MCT) as the large-scale thrusts trending towards NE–SW and NW–SE direction over the study area. The Gandak River was following the Gandak fault trending to NW–SE and also Lumbini, Thakkola Graben and Kathmandu Fault trending towards NE–SW. The Gandak mega fan, viz. Rapti, Gandak and Ghaghara-Ganga

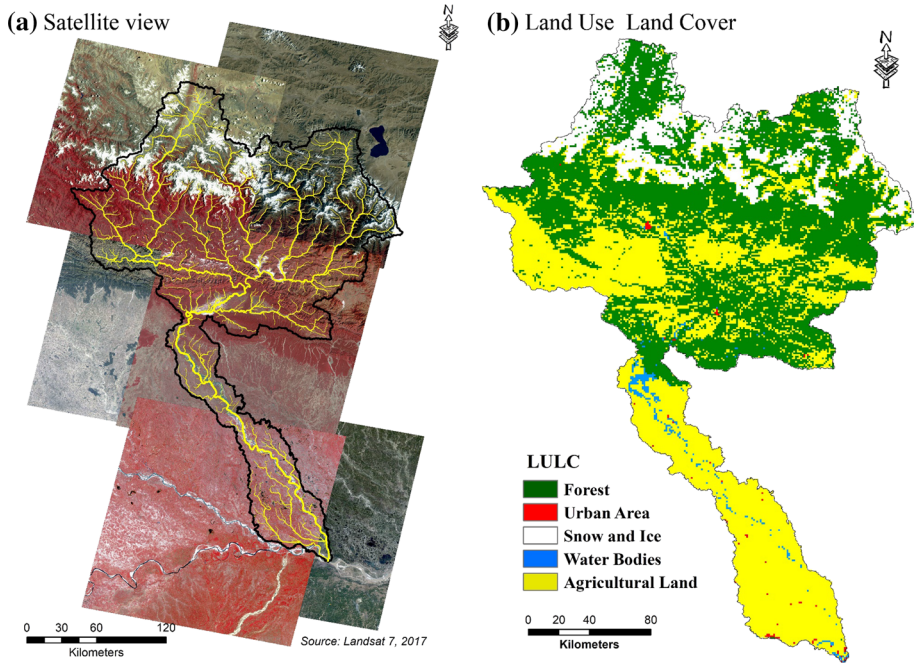

Fig. 2 Satellite view (**a**) and LULC (**b**) for the Gandak River Basin

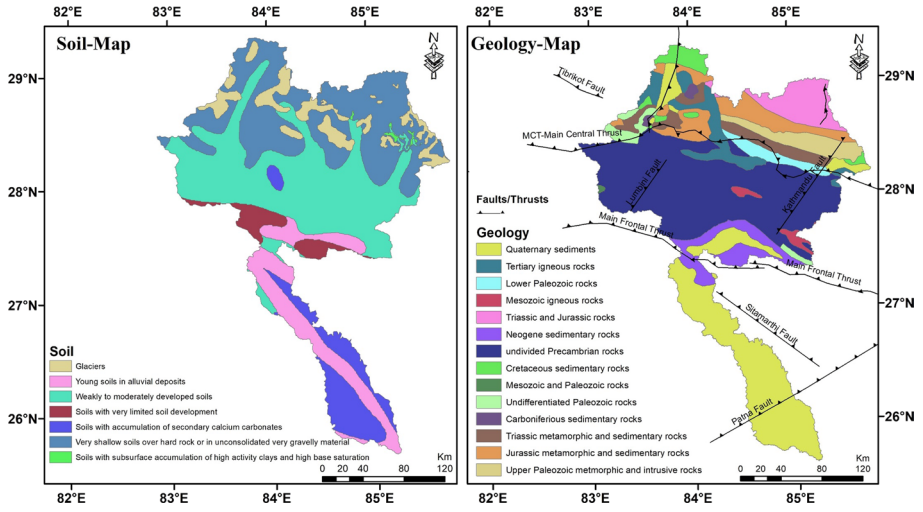

Fig. 3 Soil and geological variability maps with lineaments over the study area

(WNW-ESE) faults, may be controlling the Gandak river flow in the India. According to Sinha (2005), the most of the channel movements in this area, viz. avulsions, cut-offs, are due to the neo-tectonics and sedimentological readjustments. The study area belongs to the Himalayan region where Neo-tectonic activities mostly occur, which resulted in unstable

Table 1 Drainage morphometric parameters computed for the Gandak River Basin

Stream property	Formula	Reference	Main River	Gandak River (India)	Kali-Gandaki	Seti-Gandaki	Marsyangdi (Daraudi)	Burhi Gandak	Trishuli	East Rapti
Linear aspect										
Bifurcation ratio (R_b)	$R_b = Nu/Nu + 1$	Schumm (1956)	3.99	3.72	4.02	4.06	4.41	3.63	4.75	4.32
Rho coefficient (ρ)	R_L/R_b	Horton (1945)	0.18	3.64	0.14	0.19	0.17	0.26	0.12	0.11
Relief aspects										
Total basin relief (H) m	$H = Z - z$	Strahler (1952)	8105	1885	7955	7716	7822	7669	7040	2443
Relief ratio (R_{hl})	$R_{hl} = H/L_b$	Schumm (1956)	18.01	4.09	53.09	56.85	46.01	47.92	30.12	17.88
Ruggedness number (R_n)	$R_n = D_d * (H/1000)$	Strahler (1957)	2.86	0.78	2.75	2.72	2.53	2.65	2.40	1.04
Areal aspect										
Form factor ratio (F_f)	$F_f = A/(L_b)2$	Horton (1932)	0.22	0.05	0.53	0.16	0.17	0.20	0.12	0.17
Shape factor ratio (S_f)	$S_f = (L_b)2/A$	Horton (1932)	4.52	20.17	1.89	6.24	6.02	5.11	8.25	6.06
Elongation ratio (R_e)	$R_e = 2/L_b * (A/\pi)0.5$	Strahler (1964)	0.53	0.25	0.82	0.45	0.46	0.50	0.39	0.46
Circularity ratio (R_c)	$R_c = 12.57 * (A/P2)$	Miller (1953)	0.14	0.06	0.13	0.23	0.21	0.20	0.14	0.20
Compactness coefficient (C_c)	$C_c = 0.2841 * P/(A)\ 0.5$	Gravelius (1914)	2.70	4.24	2.75	2.11	2.21	2.28	2.67	2.24
Standard sinuosity index (S_{si})	$S_{si} = C_i/V_i$	Muller (1968a, b)	1.73	1.27	0.58	1.31	1.40	1.22	1.27	1.27

Table 1 (continued)

Stream property	Formula	Reference	Main River	Gandak River (India)	Kali-Gandaki	Seti-Gandaki	Marsyangdi (Daraudi)	Burhi Gandak	Trishuli	East Rapti
Length of overland flow (L_g) Kms	$L_g = A/2 * Lu$	Horton (1945)	1.41	1.21	1.45	1.42	1.55	1.45	1.46	1.18
Texture ratio (R_t)	$R_t = N1/P$	Schumm (1956)	1.71	0.48	0.78	0.52	0.64	0.61	0.57	0.55
Drainage density (D_d) Km/Kms^2	$D_d = Lu/A$	Horton (1932)	0.35	0.41	0.35	0.35	0.32	0.35	0.34	0.43
Stream Frequency (Fs)	$F_s = Nu/A$	Horton (1932)	0.09	0.09	0.09	0.09	0.09	0.09	0.09	0.10
Drainage intensity (D_i)	$D_i = F_s/D_d$	Faniran (1968)	2.83	0.22	2.89	2.83	3.09	2.89	2.93	2.35
Drainage pattern (D_p)	GIS software	Horton (1932)	Dendritic to circular–rectangular	Straight to dendritic	Circular to rectangular-dendritic	Dendritic	Circular		Dendritic to circular	

slopes and loose rocks. These effects play a vital role in high sediment load in the river basin. In the South-Eastern Nepal region, the sedimentation type (Bhabhar) is relatively high. Therefore, the downstream channels are generally impacted with frequent and severe flooding (IIT Kanpur 2018).

3.2 Quantitative morphometry analysis

Morphometric analysis of the GRB has been performed by using SRTM DEM data in Arc GIS 10.3 program. The determination of river flow direction, accumulation and stream order is also carried out through the DEM data. The quantitative drainage network analysis can be directly related to flooding in GRB. The different aspects of morphometry parameter such as linear, aerial and relief are calculated. Moreover, to understand the tilting and shifting of the river both transverse topography asymmetry and asymmetry factor (AF) are calculated as shown in Tables 1, 2 and 3.

3.3 Nonparametric Mann–Kendall (M–K) trend tests

The nonparametric M–K test is a tool for determining monotonic trend and rank correlation between the rank observation and their time order (Mann 1945; Kendall 1975). The statistic S of the M–K test can be calculated according to Eq. 1:

$$S = \sum_{k=1}^{n-1} \sum_{j=k+1}^{n} \mathrm{Sgn}\left(x_j - x_k\right) \tag{1}$$

where

$$\mathrm{Sgn}\left(x_j - x_k\right) = \begin{cases} 1, & \text{if}\left(x_j - x_k\right) > 0 \\ 0, & \text{if}\left(x_j - x_k\right) = 0 \\ -1, & \text{if}\left(x_j - x_k\right) < 0 \end{cases}$$

The normal distribution of the statistics S provides the Z-transformation as Eq. 2:

Table 2 Calculation of compound factor and prioritized ranks

S.No	Watersheds	R_b	D_d	Fu	T	L_o	R_f	B_s	R_e	C_c	R_c	Compound factor	Prioritized ranks
1	Gandak (Indian region)	6	2	5	7	7	7	7	7	7	1	5.6	7
2	Kali-Gandaki	5	4	6	1	3	1	1	1	6	2	3	1
3	Seti-Gandaki	4	3	2	6	5	5	5	5	1	7	4.3	5
4	Marsyangdi	2	6	3	2	1	3	3	3	2	6	3.1	2
5	Burhi Gandak	7	5	4	3	4	2	2	2	4	4	3.7	4
6	Trishuli	1	7	7	4	2	6	6	6	5	3	4.7	6
7	East Rapti	3	1	1	5	6	4	4	4	3	5	3.6	3

Table 3 Transverse topography asymmetry of the Gandak River Basin and sub-basins

Seg-ment	D_a							D_d							Transverse topography asymmetry						
	GA	W1	W2	W3	W4	W5	W6	GA	W1	W2	W3	W4	W5	W6	GA	W1	W2	W3	W4	W5	W6
A	10.17	2.46	4.66	8.38	7.48	4.43	2.53	37.65	29.3	19.91	38.97	30.78	19.63	21.49	0.27	0.08	0.23	0.21	0.24	0.22	0.12
B	49.88	1.11	4.18	3.88	4.43	5.48	2.46	113.82	26.56	15.72	17.63	18.59	28.69	13.44	0.44	0.04	0.26	0.22	0.24	0.19	0.18
C	91.79	6.25	0.53	9.02	2.22	7.25	5.23	120.65	32.68	6.53	18.83	10.65	15.6	19.39	0.76	0.19	0.08	0.48	0.20	0.46	0.27
D	9.05	4.76				4.69	2.53	13.34	54.99				27.91	21.49	0.68	0.09	0.23	0.21			
E	1.71	4.33						17.78	18.2						0.09	0.23		0.22			
F	5.07							8.03							0.63			0.47			
G	24.8							20.92							1.18						
H	13.74							26.19							0.52						

$$Z_{\mathrm{mk}} = \begin{cases} s - 1/\sigma^2, & \text{if } S > 0 \\ 0, & \text{if } S = 0 \\ s + 1/\sigma^2, & \text{if } S < 0 \end{cases} \tag{2}$$

Increasing and decreasing trends of data were decided by the positive and negative values of Z_{MK}, while trend of magnitude can be estimated by Sen's slope (Sen 1968) as

$$T_i = x_j - x_k/j - k, \quad \text{For } i = 1, 2...N \tag{3}$$

where datasets values x_j and x_k are at time j and k, respectively.

The slope of the Sen's estimator evaluated from the T_i as the median of N values can be represented by:

$$Q_i = \begin{cases} T_{N+1/2}, & N \text{ is odd} \\ \frac{1}{2}\left(T_{\frac{N}{2}} + T_{\frac{N+2}{2}},\right) & N \text{ is even} \end{cases} \tag{4}$$

In the end, Q_{median} can be calculated by a two-tailed test at 100 $(1-a)\%$ confidence interval and then a true slope can be achieved by the nonparametric test. Positive and negative results of $\mathrm{Q_i}$ state the increasing and decreasing trends of the datasets.

3.4 Standardized precipitation index (SPI)

The SPI can be calculated from rainfall by fitting to a probability distribution function. Let x be the rainfall at the chosen timescale then probability density function satisfying gamma distribution was estimated by using Eq. 5:

$$F(x) = \frac{1}{\beta^{\alpha} * \tau(\alpha)} x^{(A-1)} * e^{-\left(\frac{x}{B}\right)}, \quad x > 0 \tag{5}$$

The historical rainfall data of the station were fitted to a gamma distribution parameters shape (α) and scale (β), respectively, through a process of maximum likelihood methods in reference of estimated values of A and B, well signified by a mathematical cumulative probability function. Whereas, cumulative probability distribution to shape on the standard normal distribution to generate SPI value (McKee et al. 1993) (Table 5).

3.5 Rainfall anomaly index (RAI)

According to Van Rooy (1965), rainfall anomaly index (RAI) provides the rank of the rainfall values to find both positive and negative rainfall anomalies.

$$\mathrm{RAI} = \pm\mathrm{SF} * \left[\left(p_i - \overline{p}\right) \div \left(\overline{m} - \overline{p}\right)\right] \tag{6}$$

where p_i is total sum of rainfall for month i, $\overline{p}$ is the long-term average rainfall, $\overline{m}$ is the mean of the ten highest or lowest values of precipitation (p), $\pm$SF represent the arbitrary threshold values of $+3$ and -3 that have, respectively, been assigned to the mean of the ten most extreme positive and negative anomalies (Table 5). The rainfall anomaly is the percentage departure of monthly rainfall from the long-term mean which provides a dimensionless measure of the abnormal precipitation (Bhalme and Mooley 1980).

4 Result and discussions

The quantitative morphometric analysis is generally provided in three categories, viz. linear, areal and relief with seventh-order stream networks and fourth–sixth-order sub-basins. The other parameters were analysed for subsurface topography and geology such as transverse topographic asymmetry and asymmetry factor (Fig. 4). Extreme weather events in terms of rainfall anomaly are examined for monsoon months (JJAS) for assessing the flood events (Fig. 5). The regression model and rainfall anomaly index (RAI) were used in comparison with SPI as illustrated in Figs. 6, 7 and 8.

4.1 Network analysis (drainage)

4.1.1 Linear aspects

Stream order (S_u) classification has been done based on the Strahler's (1964) scheme for stream ordering (Table 1). It was observed that in first-order streams (higher), the hilly region pointed on terrain complexity with compact bedrock lithology in the study area (Fig. 4b). Six sub-watersheds followed the fifth stream order, while Gandak River is having seventh order of the stream. Kali-Gandaki basin was the longest stream of sub-watershed, while East Rapti was the shortest stream length. Higher values of first-order streams in GRB predict that there may be possibility of rapid flash floods followed by heavy rainfall in the downstream segments as compared to the north Ganga basin. Trishuli sub-watershed showed the highest (4.75) bifurcation ratio (R_b) between first and second orders of streams, while the R_b showed an accelerated erosion in the catchment area and that reflected of the variability in shape of stream network (Verstappen 1983; Shukla et al. 2014). From the Kali-Gandaki to East Rapti, the R_b value was found as (3.93–4.75) can be linked to low-extended peak flow with structural disturbances and distorted drainage pattern (Table 1). The Burhi Gandak basin has the highest Rho coefficient (ρ), which facilitates the estimated

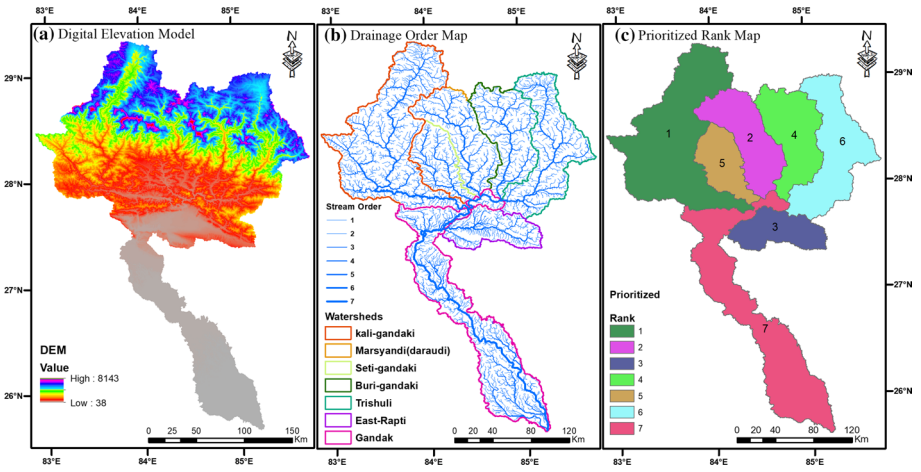

Fig. 4 Digital elevation model (**a**), drainage order map (**b**) and prioritized rank map (**c**) of the Gandak watershed

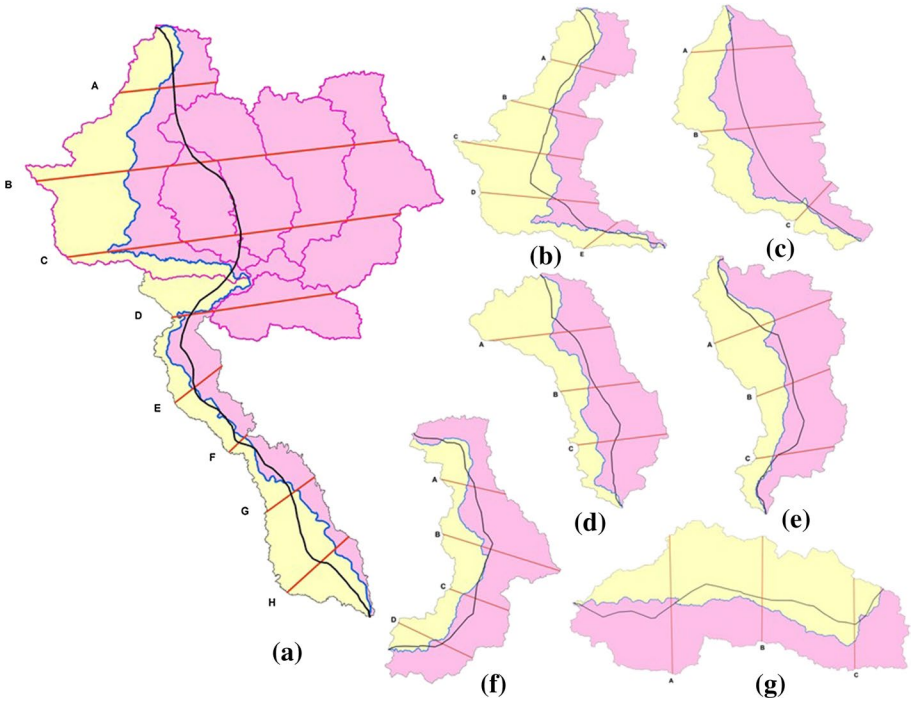

Fig. 5 Transverse topography asymmetry is demonstrating leftward shift of the channels Main Gandak River (**a**), Kali-Gandaki River (**b**), Seti-Gandaki River (**c**), Marsyangdi River (**d**), Burhi Gandak River (**e**), Trishuli-River (**f**) and East Rapti River (**g**)

storage capacity of drainage (Horton 1945). The Rho coefficient ranges from 0.11 to 0.26, which can be related to the subsurface geology. It is responsible as primary controller of the channel segments as well as higher water storage in the catchment during flooding (Shukla et al. 2014).

4.1.2 Relief aspects

Relief aspects play a significant task in drainage expansions, permeability, streamflow over the surface to sub-surface, landform development related to topography, etc. Relief (Bh) is an essential aspect for studying the denudational characteristics of the basin (Sreedevi et al. 2005). The analysis of Bh showed a very high value ranges between Kali-Gandaki (8105 m) to East Rapti (2443 m) (Table 1) (Fig. 4a). The relatively higher Relief ratio (R_{hl}) of Gandak (18.01) and its sub-watersheds (17.88–53.09) showed a steep slope and mountainous conformation of the terrain. As per Strahler (1957) method, Ruggedness number (R_n) has been calculated from the relief and drainage density (Shukla et al. 2014), which represents the structural complexity of terrain in the sub-watersheds (Table 1). The R_n of Gandak (2.86) and its six sub-watersheds was ranging from 1.04 to 2.75, which showed complexity in relief and drainage density and therefore may cause high vertical erosion in the study area.

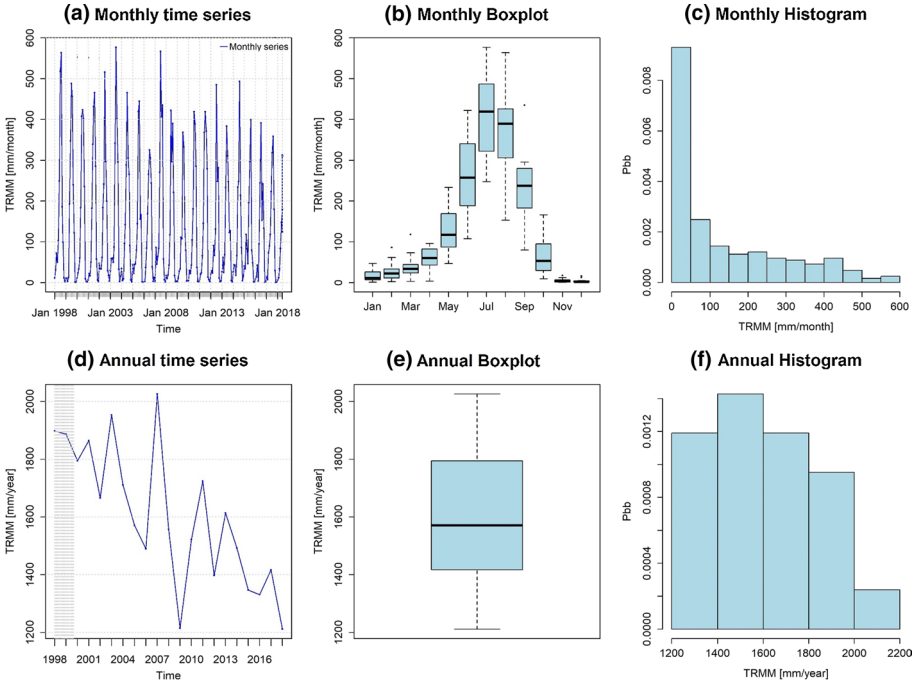

Fig. 6 Monthly and Annual rainfall (mm) time series, boxplots and histogram plots (1998 to 2018) for the Gandak River Basin, Indo-Nepal regions

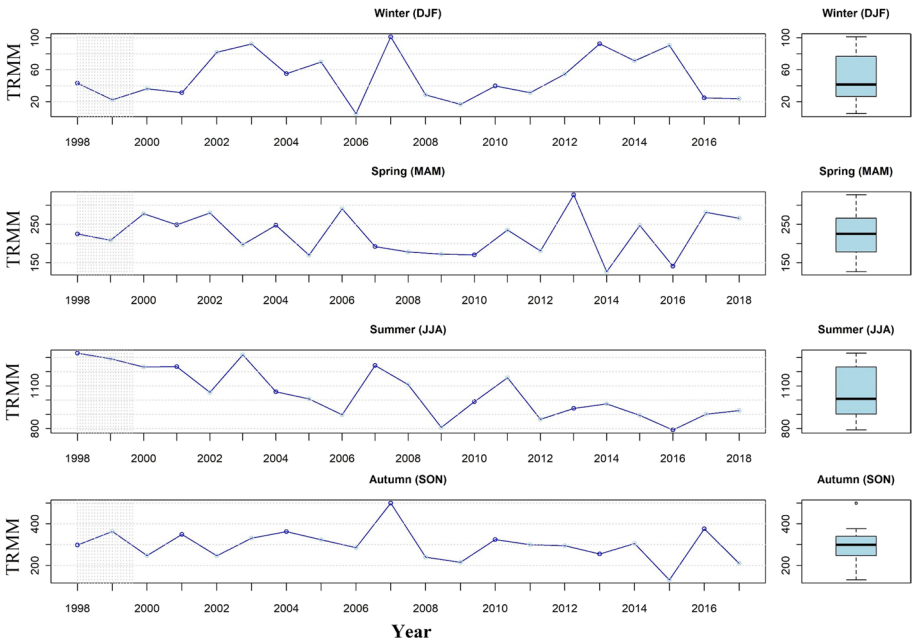

Fig. 7 Seasonal time series with boxplots of TRMM rainfall (mm) over the Gandak River Basin, Indo-Nepal regions

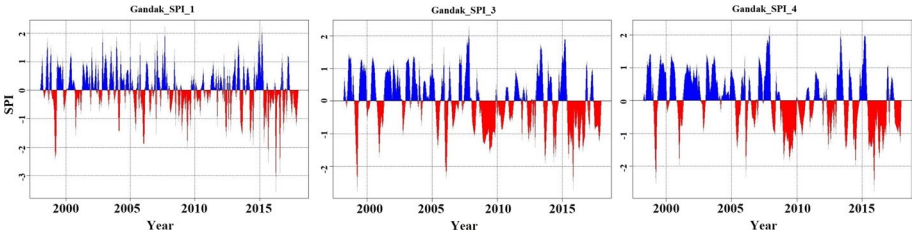

Fig. 8 Time trends of SPI_1 (monthly) (**a**), SPI_3 (winter) and (**b**), SPI_4 (monsoon) from the period of 1998–2018 over the study area

4.1.3 Areal aspects

A low drainage density (D_d) (0.35 km/sq km) has been found in GRB, which suggests an existence of moderately permeable sub-soil surface lithology and dense vegetation leads to coarse drainage texture (Table 1). The Gandak basin observed the coarse drainage texture categories controlled by climate, vegetation and lithology with the relief stage of expansion (Smith 1950; Dornkamp and King 1971). The low value ranges (1.18–1.55) of length overland flow (L_g) over Gandak and its six sub-watersheds show the occurrence of long flow paths and the area having gentle ground slopes towards the downstream, and it reflects more infiltration with sharp to short flow paths with steep ground slopes. As per Strahler (1964) method, elongation ratio (R_e) ranges between 0.20 and 1, across a broad range of climate and geologic types. For the Kali-Gandaki R_e was computed to be 0.82, which showed the watersheds vulnerability to floods (Sreedevi et al. 2005). Calculated circularity ratio (Rc) of the Gandak basin ($R_c = 0.22$) indicated an elongated nature with moderate runoff and permeability of the sub-soil. It indicates a mature stage of topography with the presence of structural disturbances (Table 1). Texture ratio (R_t) of the basin (1.71) and its sub-watersheds (0.78–0.52) showed a very high relief of the basin (Table 1). Estimated compactness coefficients (C_c) of the basin illustrated the relationship of an elongated hydrological basin. High compactness coefficient of Kali-Gandaki and GRB showed that the glaciers are very confined in the catchment area (Table 1). The Seti-Gandaki shows the highest shape factor ratio (S_f) value (6.24), and it indicates the weaker flood discharge periods in the study area (Table 1). The drainage pattern (D_p) over the catchment area showed the dendritic to rectangular drainage pattern, whereas its sub-watersheds were the circular to rectangular pattern influenced by heavy rainfall with healthy vegetation (Howard 1967). The sinuosity index (SI) of the basin and its sub-watersheds indicated that the basin is highly meandered (> 1.73) in nature, also supported by Muller (1968a, b). In addition, estimated low stream frequency (F_s) (0.09 to 0.10) and high drainage intensity (D_i) (2.35 to 3.09) could be associated with the frequent flood and channel erosion in the study area (Bhat et al. 2019).

4.2 Prioritization of sub-watersheds

Compound factor (CF) is defined as the ratio between sum of all the ranks assigned to the linear and areal parameters with the number of the parameters (Patel et al. 2013; Maurya et al. 2016; Yadav et al. 2016). Rank of the Kali-Gandaki has been assigned as first by the

way of minimum CF value as 3, while Marsyangdi (Daraudi) and East Rapti as ranking second and third, respectively (Table 2). The priority of the sub-watersheds can be specified on the basis of group of low ranking of CF, drainage density and slope while high infiltration rate (Patel et al. 2013).Water harvesting structures like check dams are suggested in sub-watersheds of Kali-Gandaki, Marsyangdi (Daraudi), East Rapti and Burhi Gandak, with priority ranks of first, second, third and fourth, respectively (Fig. 4c).

4.3 River channel shifting and trend analysis

4.3.1 Transverse topography asymmetry (T)

According to Cox et al. (2001), transverse topographic asymmetry is defined as the ratio of stream channel (D_a) and basin margin (D_d) to the middle of the basin. It means that when ratio D_a/D_d approaches 1, the stream laterally migrates towards the margin apart from centre of the basin, which indicates that lateral tilt of the river basin, while $D_a/D_d=0$ i. e. $D_a=0$, river basin would be symmetrical and its signifies that stream segment is at middle (Dhanya 2014). The average value of T was 0.57 and appeared of prominent tilt in basin (Table 3). According to previous studies for sub-basins, Kali-Gandaki River is having a low tilt, while the Gandak River is associated with high tilt (Fig. 5). The formation of the uplifted sector in the path of the river over the Indo-Nepal region by tectonic activity and inferred in the present study from Nhubine Himal Glacier to Sonepur, India (Gandak confluence with Ganga River) towards NNW to ESE direction representing the tilted basin (Fig. 5).

4.3.2 Asymmetry factor (AF)

According to Hare and Gardner 1984, AF is defined as the landscape (basin) inclination affected by confined or regional tectonic deformation over the river basin (at drainage scale), while Cox (1994) suggested that AF indicates lateral shift of river basin with respect to the main channel. AF is percentage (%) estimation of ratio between right-sided (from the main channel) downstream drainage areas (A_r) with total drainage area (A_t) of the basin (Hare and Gardner 1984; Cox 1994). The fluctuation of AF, above or below 50, resulted in direction of probable differential tilting, active tectonic/neo-tectonic activity or lithologic/structurally controlled differential erosion. The AF (> 50%) specified that the basin was slanted to the leftward, while < 50% state that the basin was slanted to the rightward with respect to the downstream direction (Hare and Gardner 1984; Molin et al. 2004). AF (30.58%) represents a negative differential value that proposed that the basin has been deviated from its original path to the right side on the way of downstream direction (Table 4). The Gandak main channel showed meander scar and growth of huge floodplain region over the downstream (India) of the channel. It is demarcated by meander cut off sand paleochannel in left bank of river basin. The catchment area of main Gandak River with its subwatersheds is having the less AF (< 50%) that pointed a channel shift to the rightward of the drainage. The sub-watersheds of Kali-Gandaki (61.82%) and East Rapti River (51.52%) basin are shifted to the leftward of the drainage basin (Fig. 5). Moreover, the Kali Gandaki and East Rapti show the uplifted characteristic in the catchment area responsible for steep runoff towards the downstream.

Table 4 Asymmetry factor parameters and asymmetry factors of the study area basin

S. No.	Basin/watersheds	A_r (Sq km)	A_t (Sq km)	AF (%)	Uplift-tilt/shift
1	Gandak River (GA)	13,712.8	44,836.148	30.58	< 50%, Right side
2	Kali-Gandaki River (W1)	7340.09	11,872.4	61.82	> 50%, Left side, uplift
3	Seti-Gandaki River (W2)	1025.78	2952.06	34.74	< 50%, Right side
4	Marsyangdi (Daraudi) River (W3)	1974.43	4796.78	41.16	
5	Burhi Gandak River (W4)	1907.11	5010.8	38.05	< 50%, Right side
6	Trishuli River (W5)	2108.77	6620.68	31.85	
7	East Rapti River (W6)	1588.24	3082.71	51.52	> 50%, Left side, uplift

Table 5 SPI and RAI classification according to their original definitions as applied in this study

S. No.	SPI (McKee et al. 1993)	Description	RAI (Van Rooy 1965)
1	≥ 2.00	Extremely wet	≥ 3.00
2	1.50 to 1.99	Very wet	2.00 to 2.99
3	1.00 to 1.49	Moderately wet	1.00 to 1.99
4	0.50 to 0.99	Slightly wet	0.50 to 0.99
5	− 0.49 to 0.49	Near normal	− 0.49 to 0.49
6	− 0.99 to − 0.50	Slightly dry	− 0.99 to − 0.50
7	− 1.49 to − 1.00	Moderately dry	− 1.99 to − 1.00
8	− 1.99 to − 1.50	Very dry	− 2.99 to − 2.00
9	≤ − 2.00	Extremely dry	≤ − 3.00

4.4 Spatial and temporal trend of rainfall for flood events

There was a vast spatial variation in rainfall found over the central part of the river basin in Nepal region. As a result, the low rainfall concentration (< 100 mm) was observed in the upper part (Trans-Himalayan ranges) of the basin, whereas the middle part witnessed a rainfall of > 700 mm/months (Fig. 6a) and 2000 (mm/year) (Fig. 6d) during monsoon season. Thus, the spatial analysis is really helpful to develop the effective watershed management plans in this region. Moreover, a distinctive spatio-temporal variation of rainfall is found in the catchment area, which added an importance to monitor the extreme events (flood) and trend in different sub-watersheds of the GRB. Twenty-year monthly and annual boxplot showed that the maximum rainfall occurred in the summer monsoon season with normal to positive distribution, while the rest of the months showed a rainfall < 250 mm/months (Fig. 6b and e). There was a systematic rise and fall observed in the rainfall trend found at the upper region of Himalaya but not clear in other physio-graphical zones over the GRB in Nepal (Panthi et al. 2015). Moreover, the central basin areas were having high rainfall in JJAS months resulting in severe flooding condition in a downward region, while areas having low rainfall could be linked with the drought condition (Dahal et al. 2016). Monthly and annual histogram plot showed that the maximum probability of rainfall in between 0 to 100 mm/month and 1400 to 1600 mm/year, respectively. Figure 7 shows that the seasonal rainfall variations in four classes as: (a) winter [December–January–February (DJF)], (b) spring [March–April–May (MAM)], (c) summer [June–July–August (JJA)]

and (d) autumn [September–October–November (SON)]. Seasonal plot helps to examine the maximum rainfall occurring in the area and can be used detect flood years. The analysis showed that the 1998, 2002, 2003, 2004, 2005, 2007, 2011 and 2013 years were having very extreme precipitation and therefore considered as flood years, also confirmed by previous studies. Maximum rainfall was examined in summer (JJA) months as above 1300 mm/year, while years 1998, 2003, 2005 and 2011 showed the maximum rainfall over the study area (Fig. 7). Box plot of the magnitude in seasonal average precipitation of spring season revealed middle clustering as normal distribution, while winter and summer rainfall distributions were median skewed towards upward (positive skewness). In the summer season, most of the extreme events come under upper quartile or in 75th percentile. Autumn (SON) month's boxplot showed downward rainfall distribution that reveals negative skewness with outliers (Fig. 7).

4.5 Standardized precipitation index (SPI) and rainfall anomaly index (RAI) for flood condition

According to van Rooy (1965) and McKee (1993) classification, the dimensionless SPI and RAI values can be classified into nine classes from extremely wet to dry followed by near normal condition (Table 5). SPI has been computed over the study area on times scale 1, 3 and 4 months, respectively, using the R language (Fig. 8). SPI_1 was the representation of the normalized distribution of monthly rainfall interpreting the frequency of extreme rainfall events in less duration of time. The northern Gandak drainages in Nepal have a SPI_1 > +2.2 pointed that the July of 2003, 2007 and August of 1998, 2015 were the very wet months. The 1-month SPI indicated a value of −2.2 in 1998 and 2001 with some higher values of -3 during December, which indicate an extremely dry condition in 2016. SPI_4 was evaluated from 4-month timescale for monsoon season and SPI_3 for the 3-month timescale for winter rainfall to estimate flooding situation in the GRB. The SPI_3 was fitted to a gamma distribution where the maximum likelihood estimation of gamma distribution parameters, α and β of the cumulative probability. SPI_4 and SPI_3 showed a large variability of extreme rainfall (flood) in 1998, 2003, 2007 (SPI_4 > 2), 2013 (SPI_4 > 1.5) and found as a wettest year (Fig. 8). In the study area, eight numbers of extreme events were estimated having the SPI value greater than 1.5 (Table 6). SPI was

Table 6 Number of extreme precipitation events as per description classification according to McKee et al. (1993) and Van Rooy (1965) over the study

Extreme condition	Description	Gandak main river	Kali-Gandaki	Marsyangdi	Burhi Gandak	East Rapti
Extremely wet	SPI ≥ 2.00	4	1	3	2	2
	RAI ≥ 3.00	2	0	1	1	3
Very wet	1.50 ≤ SPI ≤ 1.99	2	9	4	9	11
	2.00 ≤ RAI ≤ 2.99	7	10	10	7	6
Moderately wet	1.00 ≤ SPI ≤ 1.49	34	35	36	29	26
	1.00 ≤ RAI ≤ 1.99	31	31	21	30	27
Slightly wet	0.50 ≤ SPI ≤ 0.99	43	37	41	41	44
	0.50 ≤ RAI ≤ 0.99	26	26	37	34	23

assessed for estimated successive months in comparison with the previous years, which analysed the wet to dry scenario over the study area in the last twenty-one years (Fig. 8 and Fig. 9). Figure 9 represents the 4-month time trends of SPI_4 (monsoon) from the period of 1998–2018 over the sub-watersheds Kali-Gandaki, Marsyangdi, East Rapti and Burhi Gandak denoted with the priority ranks 1 to 4. The maximum number of extreme events has been found in East Rapti, while Marsyangdi sub-watersheds showed the least events (Table 6). Marsyangdi sub-watersheds showed the highest number of extremely wet (SPI ≥ 2.00) events (Fig. 9).

The RAI has been calculated for the study area as per Van Rooy (1965). As per estimated RAI greater than three revealed that extremely wet events in East Rapti and Marsyangdi sub-watersheds rather than remaining all watersheds. The highest number of extremely wet events was found in the East Rapti River (Table 6). Estimated RAI showed that the November 2002 and September 2007 were the most common period responsible for extremely wet to very wet conditions in the Gandak and its all four prioritized sub-watersheds (Fig. 10). Additionally, the long-term monsoon season (JJAS) rainfall anomaly was calculated from the extracted precipitation values over the study area for both the region of India and Nepal (Fig. 11a, b).

4.6 Comparison between extreme Precipitation indices

Precipitation indices as SPI and RAI were computed and compared for the available satellite precipitation datasets for period 1998–2018. Figure 10 signifies the monsoon variability of both the indices (timescale, 4 months) as the RAI and SPI curves are comparable. Considerable deviations occur only for the most extreme wet events, e.g. July 2002 (RAI ≥ 3.9) and 2003 (RAI ≥ 4.2), while December 2007 (2.3 ≤ SPI ≤ 2.5) for East Rapti and Marsyangdi sub-watersheds (Table 6).

4.6.1 Mann–Kendall (M–K) trend test

Trend test analysis has been performed using the M–K test to the calculated anomaly of the extracted precipitation along with the Sen's slope (Q) for twenty-one years (1998–2018). In

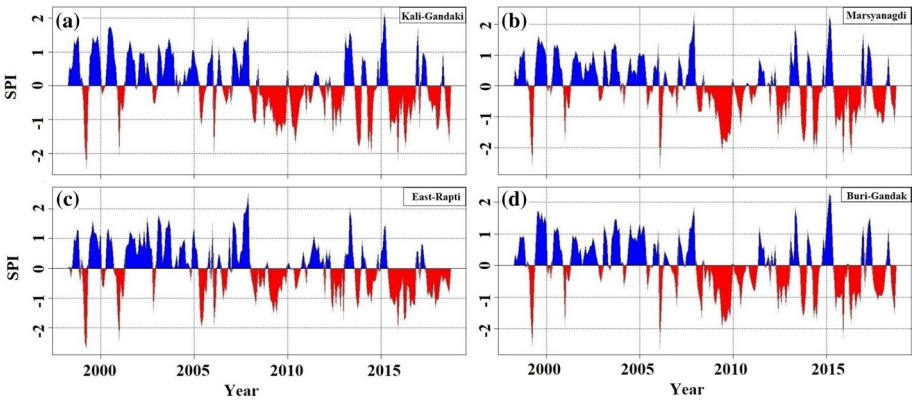

Fig. 9 Time trends of SPI_4 (monsoon) from the period of 1998–2017 over the sub watersheds Kali-Gandaki (**a**), Marsyangdi (**b**), East Rapti (**c**) and Burhi Gandak (**d**)

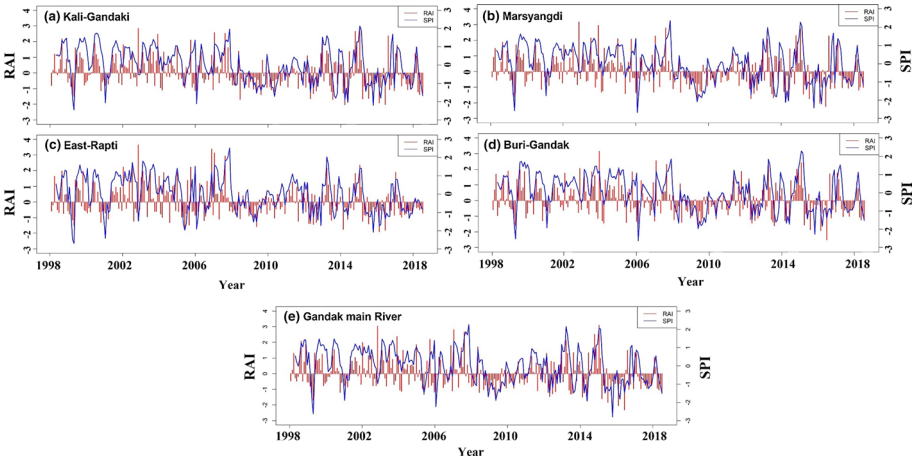

Fig. 10 Comparison of SPI and RAI at 4-monthly timescales from period 1998–2018 averaged over the study area

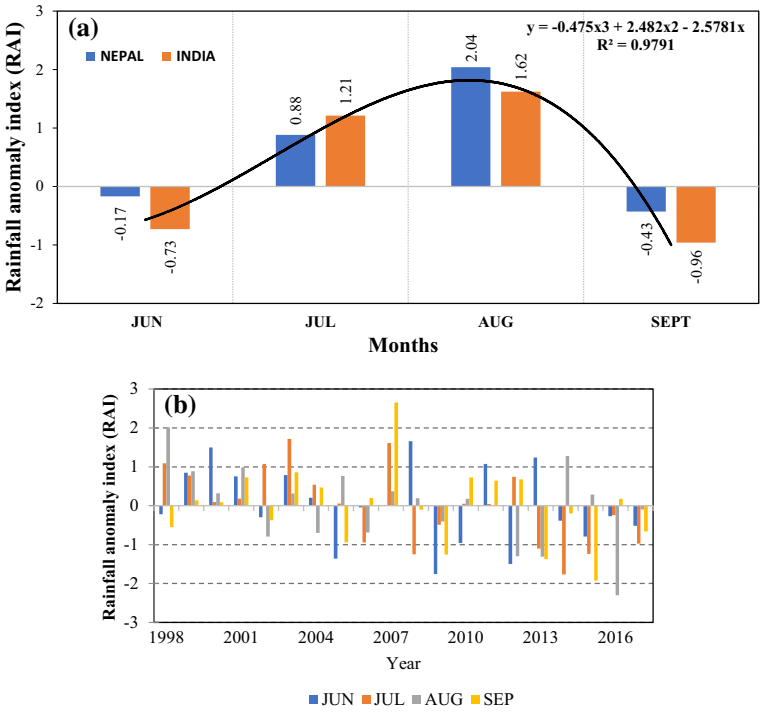

Fig. 11 Rainfall anomaly index (1998 to 2018) for the average (**a**) and monthly (**b**), JJAS over the Indo-Nepal regions

the M–K test, Z_c statistics ranges from 0.891 to − 0.48, which indicates a rising and declining trend in the GRB. The M–K test has been computed at the confidence level ($p < 0.05$). The yearly estimation of Sen's slope (Q) shows a rising slope in flood years 1998 (8.15)

and 2001 (5.21). In overall, long-term rainfall trend by M–K test showed a negative trend (−0.573). Applied M–K test over the estimated SPI and RAI provided tau values of −0.13 and −0.24, respectively, which is found highly significant with the p value ≤ 0.001. The calculated correlation coefficient of 0.526 has been found between RAI and SPI values (Fig. 12). Among different watersheds, the prioritized sub-watersheds Kali-Gandaki and Burhi Gandak showed the highest correlation coefficients with the values of 0.54 and 0.53, respectively. The hypothesis tests with the Pearson correlation is executed at a 95% confidence interval which is statistically significant at the p-value of < 0.05.

4.7 Potentially hazardous physical conditions of the basin and extreme events

The morphometric parameters and extreme weather events are taken into consideration to assess the flood influencing characteristics in GRB and each prioritized sub-watershed. The GRB is found to be in high flood hazardous zone based on the mentioned datasets and methodology. As per the analysis, flood over the catchment area is affecting the agricultural crop growth and population density mainly in Paschim-Purvi Champaran, Kushinagar, Gopalganj, Muzaffarpur and Vaishali districts of Bihar (India). Recently, Burhi Gandak has experienced flooding during August 2017 (GFCC 2018). The stream number showed a very high value in first-order streams, which stated extreme flood event in less duration of time. The calculation of four month's (monsoon) timescale SPI and RAI also confirmed the findings of the extreme events in the basin. Marsyangdi and Burhi Gandak sub-watersheds showed the maximum rate of extreme weather events evaluated from SPI (≥ 2) and RAI (≥ 3). Both the watersheds are having a low value of drainage density could be due to sparse vegetation and mountainous relief. The variability in relief condition may cause high runoff and erosion, which may lead to severe flood in the downstream area (low altitude). The high runoff responsible for flood situation and channel shifting (with the formation of paleo-channels) was calculated from precipitation indices and asymmetric factors, respectively, over the flood-affected districts of the study area. The maximum discharge of the river has been recorded as 11,400 m^3/s at Dumariaghat and 13,250 m^3/s at Triveni in 2007 (CWPRS 2012). The variability of relief condition can increase the runoff, and

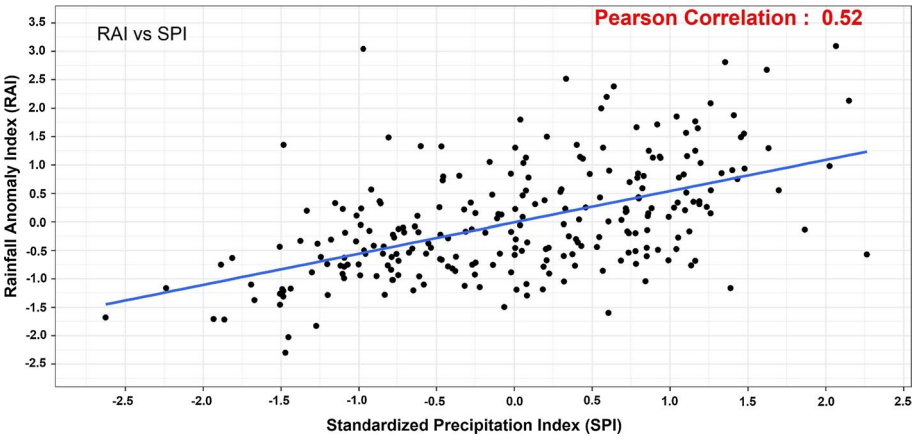

Fig. 12 Scatterplot with Pearson correlation between estimated extreme indices at 95% confidence level over study area

erosion resulted in a severe flood condition in the downstream area (low altitude). The high circulatory ratio of mountainous prioritized sub-watersheds Marsyangdi, Burhi Gandak and East Rapti, may lead to high flood risk during peak time of rainfall, while high shape factor and drainage intensity are associated with the channel erosion. The climate in each of the four prioritized sub-watersheds is either arid or semi-arid with highest monthly precipitation of 747 mm in East Rapti and average of monthly sum precipitation ranging from 101 to 169 mm per year in the GRB. The high intensity of precipitation over the risky area can result in high runoff in the basin. The extreme events could affect the Indian region and disrupt kharif season crops cultivated in the Bihar state in India.

4.8 Possible uncertainties

Uncertainty analysis is generally used to know or uncover the ambiguity associated with the variables and provide confidence in the decision-making process. The knowledge base of the system is represented by models and ground observations for, e.g. in our case the DEM data used for morphometric analysis, precipitation datasets from satellite and the methodology implemented for extreme events. In our study, SRTM DEM is used for morphometric analysis. Although it is not the best DEM for morphometric analysis, results are quite satisfactory when used for basin level analysis. Studies by Szabo et al. 2015 compared the two freely available global DEM, i.e. ASTER GDEM and SRTM, and demonstrated that SRTM is better in terms of error variance. They found an uncertainty in the mean difference between topographic elevations of SRTM-V2, SRTM-V3 and GDEM ± 4 m, ± 2.5 m and 9.1 m, respectively. For extreme precipitation events, TMPA satellite data were used. Spatial resolution of satellite product used in this study is in the order of approx. 27.75 km. Although the precipitation data are of course resolution, for basin level analysis results are generally good with low errors. Many researchers used and compared the TMPA precipitation and provided that the data are good and can be used for hydro-meteorological studies. Study indicated that the TMPA provides a good performance at monthly scales. It successfully reproduces the ground-based histogram of precipitation and is able to detect large daily events (Huffman et al. 2007). Similarly, the study by Prakash et al. over Indian region demonstrated that both research and near real-time TMPA are giving satisfactorily high-performance during monsoon as compared to Global Satellite Mapping of Precipitation (GSMaP). For trend and pattern analysis, the MK test is very powerful, but some error in estimate may occur when there are periodicities (i.e. seasonal effects) in the data (Hirsch et al. 1991). In order to minimize the uncertainty due to this, all possible known periodic effects have been removed during preprocessing of the data. In order to get the maximum advantage of MK test, a longer time series is used in this study, as it gives more negative results in shorter datasets. On the other hand, Sen is a robust method and less suffered by extreme and missing values (Sicard et al. 2011).

5 Conclusions

The study has demonstrated the use of geospatial technique for extreme events assessment through morphometric analysis and long-term rainfall datasets. This study analysed monthly and seasonal RAI and SPI values calculated from long-term rainfall data and estimated the shift in the frequency of precipitation anomaly. Morphometric analysis, geology, soil, LULC indicated a less infiltration rate, which could be the reason for a high runoff in

the basin and related flood. The flooding in GRB can be linked to the different triggering factors, i.e. stream number (high value of first-order), Rho coefficient (high), Melton ruggedness number (high), elongation ratio (less), shape factor (high) and drainage intensity (low), etc. It has been perceived that the low drainage density causes a high residence time of the water that leads to flooding like situation in the basin. Besides, there was a large inter-annual variation with distinct trends of rainfall in the monsoon season (JJAS) over the study region. The monsoon, winter and annual SPI trend reveal the extreme weather events (flood) based on the long-term analysis can be observed in the years 1998, 2002, 2007, 2011, 2013 and 2017. An analysis of flood years indicated a high SPI and RAI anomalies, which confirms these findings. Precipitation trends estimated by M–K test indicated an increasing trend of precipitation during flood years and wet season in last two decades. The RAI and SPI were calculated, which revealed a high correlation on monthly and seasonal timescales. The high rate of flood events was examined in prioritized sub-watersheds kali-Gandak, Marsyangdi, East Rapti and Burhi Gandak, which are vulnerable to extreme hydrological events such as intense rainfall and flood and therefore need utmost attention for soil and water conservation. The prioritization of watersheds will support decreasing the runoff and could control flood in the basin. Therefore, the outcome of this study can be used to develop suitable water management practices for a better planning and development of flood mitigation in the GRB.

Acknowledgements Authors are thankful to CGIR-CSI for providing SRTM based Digital Elevation Model used in study. We also acknowledge NASA-JAXA (TRMM) for providing rainfall datasets used in the study. Authors are grateful to the DST-Mahamana Centre of Excellence in Climate Change Research funded by Department of Science and Technology, New Delhi, Climate Change Programme for providing scientific and technical support.

Funding Authors thank the Climate Change Programme, Department of Science and Technology, New Delhi, for financial support (DST/CCP/CoE/80/2017(G)).

Compliance with ethical standards

Conflict of interest The authors declare no conflict of interest.

References

Abdulkareem, J. H., Sulaiman, W. N. A., Pradhan, B., & Jamil, N. R. (2018). Relationship between design floods and land use land cover (LULC) changes in a tropical complex catchment. *Arabian Journal of Geosciences, 11*(14), 376. https://doi.org/10.1007/s12517-018-3702-4.

Bhalme, H. N., & Mooley, D. A. (1980). Large-scale droughts/floods and monsoon circulation. *Monthly Weather Review, 108*(8), 1197–1211. https://doi.org/10.1175/1520-0493(1980)108<1197:LSDAMC>2.0.CO;2.

Bhatt, D., & Mall, R. K. (2015). Surface water resources, climate change and simulation modeling. *Aquatic Procedia, 4*, 730–738. https://doi.org/10.1016/j.aqpro.2015.02.094.

Bhat, M. S., Alam, A., Ahmad, S., et al. (2019). Flood hazard assessment of upper Jhelum basin using morphometric parameters. *Environmental Earth Sciences, 78*, 54. https://doi.org/10.1007/s12665-019-8046-1.

Chaubey, P. K., Kundu, A., & Mall, R. K. (2019). A geo-spatial inter-relationship with drainage morphometry, landscapes and NDVI in the context of climate change: a case study over the Varuna river basin (India). *Spatial Information Research, 27*, 627–641. https://doi.org/10.1007/s41324-019-00264-2.

Choudhari, P. P., Nigam, G. K., Singh, S. K., & Thakur, S. (2018). Morphometric based prioritization of watershed for groundwater potential of Mula river basin, Maharashtra, India. *Geology, Ecology, and Landscapes, 2*(4), 256–267. https://doi.org/10.1080/24749508.2018.1452482.

Clarke, J. I. (1966). Morphometry from maps. *Essays in geomorphology, 252*, 235–274.

Cox, R. T. (1994). Analysis of drainage-basins symmetry as rapid technique to identify areas of possible Quaternary tilt-block tectonics: an example from Mississippi Embayment. *Geological Society of America Bulletin, 106*(5), 571–581. https://doi.org/10.1130/0016-7606(1994)106<0571:AODBSA>2.3.CO;2.

Cox, R. T., Van Arsdale, R. B., & Harris, J. B. (2001). Identification of possible Quaternary deformation in the northeastern Mississippi Embayment using quantitative geomorphic analysis of drainage-basin asymmetry. *Geological Society of America Bulletin, 113*(5), 615–624.

CWPRS (2012). *Central work and power Research Station*. Government of India, Ministry of water resources, Technical Report No. 5015

Dahal, P., Shrestha, N. S., Shrestha, M. L., Krakauer, N. Y., Panthi, J., Pradhanang, S. M., et al. (2016). Drought risk assessment in central Nepal: temporal and spatial analysis. *Natural Hazards, 80*(3), 1913–1932. https://doi.org/10.1007/s11600-018-0121-6.

Deo, R. C., Byun, H. R., & Adamowski, J. F. (2015). A real-time flood monitoring index based on daily effective precipitation and its application to brisbane and Lockyer valley flood events. *Water, 29*, 4075. https://doi.org/10.1007/s11269-015-1046-3.

Dey, S., Bhatt, D., Haq, S., & Mall, R. K. (2020). Potential impact of rainfall variability on groundwater resources: a case study in Uttar Pradesh, India. *Arabian Journal of Geosciences*. https://doi.org/10.1007/s12517-020-5083-8.

Dhanya, V. (2014). Basin asymmetry and associated tectonics: a case study of Achankovil river basin, Kerala. *Transactions of the Institute of Indian Geographers, 36*, 207–215.

Dornkamp, J. C., & King, C. A. M. (1971). *Numerical analyses in geomorphology, an introduction* (p. 372). New York: St. Martins Press.

Dwivedi, G. N., Sharma, S. K., Prasad, S., & Rai, R. P. (1997). Quaternary geology and geomorphology of a part of Ghaghara-Rapti-Gandak sub-basins of Indogangetic Plain, Uttar Pradesh. *Journal of the Geological Society of India, 49*(2), 193–202.

Edon, M., & Singh, S. K. (2019). Quantitative estimation of soil erosion using open access earth observation data sets and Erosion Potential Model. *Water Conservation Science and Engineering*. https://doi.org/10.1007/s41101-019-00078-1.

Faniran, A. (1968). The index of drainage intensity—a provisional new drainage factor. *Australian Journal of Science, 31*, 328–330.

GFCC (2018). Ganga Flood Control Commission (GFCC): Annual report 2017–18. Government of India Ministry of Water Resources, River Development & Ganga Rejuvenation Ganga Flood Control Commission, Patna. https://gfcc.bih.nic.in/Docs/GFCC-AR-2017-18-EN.pdf. Accessed 14 January 2020

Gravelius, H. (1914). Flusskunde. GoschenVerlagshandlung berlin. In Zavoianu I (Ed.), 1985. Morphometry of drainage basins. Amsterdam: Elsevier.

Gupta, M., Srivastava, P. K., Islam, T., & Ishak, A. M. B. (2013). Evaluation of TRMM rainfall for soil moisture prediction in a subtropical climate. *Environmental Earth Sciences*. https://doi.org/10.1007/s12665-013-2837-6.

Hare, P.W., & Gardner, T.W. (1984). Geomorphic indicators of vertical neo-tectonism along converging plate margins, Nicoya Peninsula, Costa Rica. In M. Morisawa & J. T. Hack (Eds.), *Proceedings of 15th geomorphology symposium on tectonic geomorphology* (pp. 76–104). Birmingham, Allen &Unwinr, Boston.

Hirsch, R. M., Alexander, R. B., & Smith, R. A. (1991). Selection of methods for the detection and estimation of trends in water quality. *Water Resources Research, 27*, 803–813.

Horton, R. E. (1932). Drainage-basin characteristics. *Eos, Transactions American Geophysical Union, 13*(1), 350–361. https://doi.org/10.1029/TR013i001p00350.

Horton, R. E. (1945). Erosional development of streams and their drainage basins hydrophysical approach to quantitative morphology. *Bulletin of the Geological Society of America, 56*(3), 275–370. https://doi.org/10.1177/030913339501900406.

Howard, A. D. (1967). Drainage analysis in geologic interpretation: a summation. *AAPG bulletin, 51*, 2246–2259.

Huffman, G. J., Bolvin, D. T., Nelkin, E. J., Wolff, D. B., Adler, R. F., Gu, G., et al. (2007). The TRMM multisatellite precipitation analysis (TMPA): quasi-global, multiyear, combined-sensor precipitation estimates at fine scales. *Journal of hydrometeorology, 8*(1), 38–55.

IIT Kanpur (2018). Interfan area. Geology. https://www.iitk.ac.in/gangetic. Accessed 20 June 2018.

Kendall, M. G. (1962). Rank correlation methods. *Journal of American Statistical Association, 63*(324), 1379–1389. https://doi.org/10.1080/01621459.1968.10480934.

Kumar, N., Singh, S. K., & Pandey, H. K. (2018). Drainage morphometric analysis using open access earth observation datasets in a drought-affected part of Bundelkhand, India. *Applied Geomatics, 10*(3), 173–189. https://doi.org/10.1007/s12518-018-0218-2.

Malik, S., Pal, S. C., Sattar, A., Singh, S. K., Das, B., Chakrabortty, R., et al. (2020). Trend of extreme rainfall events using suitable global circulation model to combat the water logging condition in Kolkata metropolitan area. *Urban Climate*. https://doi.org/10.1016/j.uclim.2020.100599.

Mall, R. K. (2013). Climate change and water security: an Indian perspective. *Signatures, Newsletter of the ISRS-AC, 25*, 119–133.

Mall, R. K., & Srivastava, R. K. (2012). Sustainable flood management in changing climate. In O. P. Mishra, M. Ghatak, & A. Kamal (Eds.), *Flood risk management in South Asia* (pp. 49–66). New Delhi: SAARC Disaster Management Centre.

Mall, R.K., Gupta, A., Singh, R., Singh, R.S. & Rathore, L.S. (2006). Water resources and climate change: an Indian perspective. Current science, pp. 1610–1626.

Mall, R. K., Attri, S. D., & Kumar, S. (2011a). Extreme weather events and climate change policy in India. *Journal of South Asian Studies, 4*, 27–76.

Mall, R. K., Kumar, R., & Bhatla, R. (2011b). Climate change and disaster in India. *Journal of South Asian Disaster Studies, 4*(1), 27–76.

Mall, R. K., Srivastava, R. K., Banerjee, T., Mishra, O. P., Bhatt, D., & Sonkar, G. (2019). Disaster risk reduction including climate change adaptation over south Asia: challenges and ways forward. *International Journal of Disaster Risk Science, 10*, 14–27. https://doi.org/10.1007/s13753-018-0210-9.

Mann, H. B. (1945). Nonparametric tests against trend. *Econometrica, 13*(3), 245–259.

Maurya, S., Srivastava, P. K., & Gupta, M. (2016). Integrating soil hydraulic parameter and microwave precipitation with morphometric analysis for watershed prioritization. *Water Resources Management, 30*, 5385. https://doi.org/10.1007/s11269-016-1494-4.

McKee, T. B., Doesken, N. J. & Kleist, J. (1993). The relationship of drought frequency and duration to time scales. In *Proceedings of the 8th conference on applied climatology*, *17*(22), 179–183.

Meshram, S. G., Singh, S. K., Meshram, C., Deo, R. C., & Ambade, B. (2018). Statistical evaluation of rainfall time series in concurrence with agriculture and water resources of Ken River Basin, Central India (1901–2010). *Theoretical and Applied Climatology, 134*(3–4), 1231–1243. https://doi.org/10.1007/s00704-017-2335-y.

Miller, V. C. (1953). A quantitative geomorphic study of drainage basin characteristics in the clinch mountain area. Virginia and Tennessee. In *Technical report. 3. Office of naval research*. New York: Department of Geology, Columbia University, Geography Branch, 1960.

Mohindra, R., Parkash, B., & Prasad, J. (1992). Historical geomorphology and pedology of the Gandak-megafan, middle Gangetic Plains, India. *Earth Surface Processes and Landforms, 17*(7), 643–662. https://doi.org/10.1002/esp.3290170702.

Molin, P., Pazzaglia, F. J., & Dramis, F. (2004). Geomorphic expression of active tectonics in a rapidly-deforming forearc, Sila massif, Calabria, southern Italy. *American Journal of Science, 304*(7), 559–589. https://doi.org/10.2475/ajs.304.7.559.

Muller, J. E. (1968a). An introduction to the hydraulic and topographic sinuosity indexes. *Annals of the Association of American Geographers, 58*(2), 371–385.

Muller, J. E. (1968). An introduction to the hydraulic and topographic sinuosity indexes. *Annals of the Association of American Geographers, 58*(2), 371–385. https://doi.org/10.1111/j.1467-8306.1968.tb00650.x.

Nagalapalli, S., Kundu, A., Mall, R. K., Thattai, D., & Rangarajan, S. (2019). An appraisal of flood events using IMD, CRU, and CCSM4-derived meteorological data sets over the Vaigai river basin, Tamil Nadu (India). *Sustainable Water Resources Management, 5*, 1731–1744. https://doi.org/10.1007/s40899-019-00325-2.

Panthi, J., Dahal, P., Shrestha, M. L., Aryal, S., Krakauer, N. Y., Pradhanang, S. M., et al. (2015). Spatial and temporal variability of rainfall in the Gandaki River Basin of Nepal Himalaya. *Climate, 3*(1), 210–226. https://doi.org/10.3390/cli3010210.

Patel, D. P., Gajjar, C. A., & Srivastava, P. K. (2013). Prioritization of Malesari mini-watersheds through morphometric analysis: a remote sensing and GIS perspective. *Environmental Earth Sciences, 69*, 2643. https://doi.org/10.1007/s12665-012-2086-0.

Pophare, A. M., & Balpande, U. S. (2014). Morphometric analysis of Suketi river basin, Himachal Himalaya, India. *Journal of Earth System Science, 123*(7), 1501–1515. https://doi.org/10.1007/s12040-014-0487-z.

Pradhan, R. K., Srivastava, P. K., Maurya, S., Singh, S. K., & Patel, D. P. (2018). Integrated framework for soil and water conservation in Kosi River Basin through soil hydraulic parameters, morphometric analysis and earth observation dataset. *Geocarto International*. https://doi.org/10.1080/10106049.2018.1520921.

Rajeevan, M., Bhate, J., & Jaswal, A. K. (2008). Analysis of variability and trends of extreme rainfall events over India using 104 years of gridded daily rainfall data. *Geophysical Research Letters*. https://doi.org/10.1029/2008GL035143.

Rawat, K. S., Singh, S. K., Singh, M. I., & Garg, B. L. (2018). Comparative evaluation of vertical accuracy of elevated points with ground control points from ASTERDEM and SRTMDEM with respect to CARTOSAT-1DEM. *Remote Sensing Applications: Society and Environment, 13*, 289–297. https://doi.org/10.1016/j.rsase.2018.11.005.

Roorkee, N. I. H. (2017). Gandakriver. https://nihroorkee.gov.in/Gangakosh/tributaries/Gandak.htm. Accessed 20 June 2017.

Schumm, S. A. (1956). Evolution of drainage systems and slopes in badlands at Perth Amboy, New Jersey. *Geological Society of America Bulletin, 67*(5), 597–646. https://doi.org/10.1130/0016-7606.

Seiler, R. A., Hayes, M., & Bressan, L. (2002). Using the standardized precipitation index for flood risk monitoring. *International Journal of Climatology, 22*(11), 1365–1376. https://doi.org/10.1002/joc.799.

Sen, P. K. (1968). Estimates of the regression coefficient based on Kendall's tau. *Journal of the American Statistical Association, 63*(324), 1379–1389. https://doi.org/10.2307/2285891.

Shukla, D. P., Dubey, C. S., Ningreichon, A. S., Singh, R. P., Mishra, B. K., & Singh, S. K. (2014). GIS-based morpho-tectonic studies of Alaknanda river basin: a precursor for hazard zonation. *Natural Hazards, 71*, 1433. https://doi.org/10.1007/s11069-013-0953-y.

Sicard, P., Dalstein-Richier, L., & Vas, N. (2011). Annual and seasonal trends of ambient ozone concentration and its impact on forest vegetation in Mercantour National Park (South-eastern France) over the 2000–2008 period. *Environmental Pollution, 159*(2), 351–362.

Sigdel, M., & Ikeda, M. (2010). Spatial and temporal analysis of drought in Nepal using standardized precipitation index and its relationship with climate indices. *Journal of Hydrology and Meteorology, 7*(1), 59–74.

Singh, R. B., & Mal, S. (2014). Trends and variability of monsoon and other rainfall seasons in Western Himalaya, India. *Atmospheric Science Letters, 15*(3), 218–226. https://doi.org/10.1002/asl2.494.

Singh, S. K., Basommi, B. P., Mustak, S. K., Srivastava, P. K., & Szabo, S. (2018). Modelling of land use land cover change using earth observation data-sets of Tons River Basin, Madhya Pradesh, India. *Geocarto International, 33*(11), 1202–1222. https://doi.org/10.1080/10106049.2017.1343390.

Singh, V. K., Kumar, D., Kashyap, P. S., Singh, P. K., Kumar, A., & Singh, S. K. (2020). Modelling of soil permeability using different data driven algorithms based on physical properties of soil. *Journal of Hydrology, 580*, 124223. https://doi.org/10.1016/j.jhydrol.2019.124223.

Sinha, R., Tandon, S. K., Gibling, M. R., Bhattacharjee, P. S., & Dasgupta, A. S. (2005). Late quaternary geology and alluvial stratigraphy of the Ganga basin. *Himalayan Geology, 26*(1), 223–240.

Smith, K. G. (1950). Standards for grading texture of erosional topography. *American Journal of Science, 248*(9), 655–668.

Sreedevi, P. D., Subrahmanyam, K., & Ahmed, S. (2005). Integrated approach for delineating potential zones to explore for groundwater in the Pageru River basin, Cuddapah District, Andhra Pradesh, India. *Hydrogeology Journal, 13*(3), 534–543. https://doi.org/10.1007/s10040-004-0375-8.

Stankevich, S., Piestova, I., Kozlova, A., Titarenko, O., & Singh, S. K. (2020). Satellite radar interferometry processing and elevation change analysis for geo-environmental hazard assessment. In P. K. Srivastava, S. K. Singh, U. C. Mohanty, & T. Mutry (Eds.), *Techniques for disaster risk management and mitigation (geophysical monograph series)*. USA: Wiley.

Strahler, A. N. (1952). Hypsometric (area-altitude) analysis of erosional topography. *Geological Society of America Bulletin, 63*(11), 1117–1142.

Strahler, A. N. (1957). Quantitative analysis of watershed geomorphology. *Eos, Transactions American Geophysical Union, 38*(6), 913–920.

Strahler, A. N. (1964). *Quantitative geomorphology of drainage basins and channel networks. Handbook of applied hydrology* (pp. 4–39). New York: McGraw-Hill.

Szabó, G., Singh, S. K., & Szabó, S. (2015). Slope angle and aspect as influencing factors on the accuracy of the SRTM and the ASTER GDEM databases. *Physics and Chemistry of the Earth, Parts A/B/C, 83–84*, 137–145. https://doi.org/10.1016/j.pce.2015.06.003.

Van Rooy, M. P. (1965). A rainfall anomaly index independent of time and space. *Notos, 14*(43), 6.

Verstappen, H. T. (1983). Applied geomorphology. Geomorphological Surveys for environmental development No. 551.4 VER. *Progress in Physical Geography Earth and Environment*. https://doi.org/10.1177/030913338500900125.

Yadav, S. K., Singh, S. K., Gupta, M., & Srivastava, P. K. (2014). Morphometric analysis of upper tons basin from Northern Foreland of Peninsular India using CARTOSAT satellite and GIS. *Geocarto International, 29*(8), 895–914. https://doi.org/10.1080/10106049.2013.868043.

Yadav, S. K., Dubey, A., Szilard, S., & Singh, S. K. (2016). Prioritisation of sub-watersheds based on earth observation data of agricultural dominated northern river basin of India. *Geocarto International, 33*(4), 339–356. https://doi.org/10.1080/10106049.2016.1265592.